JPP Journal of Pharmacy and Pharmacology

JPP 2007, 59: 537–547

Received March 6, 2006
Accepted December 11, 2006
DOI 10.1211/jpp.59.4.0008
ISSN 0022-3573

Design, synthesis and enzymatic evaluation of 6-bridged imidazolyluracil derivatives as inhibitors of human thymidine phosphorylase

Virginia A. McNally, Mehdi Rajabi, Abdul Gbaj, Ian J. Stratford, Philip N. Edwards, Kenneth T. Douglas, Richard A. Bryce, Mohammed Jaffar and Sally Freeman

Abstract

A series of novel imidazolyluracil conjugates were rationally designed and synthesised to probe the active site constraints of the angiogenic enzyme, thymidine phosphorylase (TP, E.C. 2.4.2.4). The lead compound in the series, **15d**, showed good binding in the active site of human TP with an inhibition in the low μM range. The absence of a methylene bridge between the uracil and the imidazolyl subunits (series 16) decreased potency (up to 3-fold). Modelling suggested that active site residues Arg202, Ser217 and His116 are important for inhibitor binding.

Introduction

Thymidine phosphorylase (TP, dThPase, E.C. 2.4.2.4), which is identical to platelet-derived endothelial cell growth factor (PD-ECGF), catalyses the phosphorolysis of thymidine (**1**) to thymine (**2**) and 2-deoxyribose-1-phosphate (**3**) (Figure 1) (Krenitsky et al 1981). Early therapeutic interest in TP was associated with its catalytic conversion of the cancer chemotherapeutic drug, 5-fluorouracil (**4**, 5-FU) to its metabolite 5-fluoro-2′-deoxyuridine, which is then further metabolised to 5-fluoro-2′-deoxyuridine-1′-phosphate, the activated anti-cancer agent (Schwartz et al 1994).

TP has been associated with the bioactivation of many fluorinated anti-cancer prodrugs (Figure 2), such as 1-(tetrahydro-2-furanyl)-5-fluorouracil (**5**, Tegafur) (Kono et al 1981; Miwa et al 1986; Patterson et al 1995), 5′-deoxy-5-fluorouridine (**6**, Furtulon, doxifluridine, 5′-DFUR) (Kono et al 1983) and *N*-4-pentyloxy-carbonyl-5′-deoxy-5-fluorocytidine (**7**, capecitabine, Xeloda) (Ishikawa et al 1998). Conversely, the cytotoxicity of other anti-cancer agents, such as 2′-deoxy-5-(trifluoromethyl)uridine (**8**, F_3dThd) is reduced via an inactivation process due to the presence/over-expression of TP (Ishikawa et al 1998).

Recent literature has indicated that TP is over-expressed in many solid tumours and its over-expression is regulated by the hypoxic inducible factor 1 (HIF-1) (Griffiths & Stratford 1997; Fukushima et al 2000). Its role as a pro-angiogenic enzyme has been investigated, and studies suggest that TP is intricately involved in the growth, maintenance and promotion of metastatic tumours, especially when associated with vascular endothelial growth factor (VEGF) (Relf et al 1997; Brown & Bicknell 1998; Griffiths & Stratford 1998; Toi et al 2005). TP has been associated with the metastatic capabilities of a number of tumours, including gastric (Maeda et al 1997), bladder (O'Brien et al 1996; Shimabukuro et al 2005) and colorectal (Takebayashi et al 1996). Its over-expression has also been implicated in the growth of ovarian (Reynolds et al 1994), oesophageal and pancreatic cancers (Takao et al 1998).

Although inhibition of TP may be incompatible with the inactivation of a variety of fluoropyrimidine-based anti-cancer agents, it can be used to control the growth of tumours. This is best illustrated by the fact that one of the most potent inhibitors of TP, 5-chloro-6-[1-(2-iminopyrrolidinyl)methyl]uracil hydrochloride (**9**, TPI, Figure 3), caused a substantial reduction in tumour growth when administered to mice carrying tumours that

School of Pharmacy & Pharmaceutical Sciences, University of Manchester, Oxford Road, Manchester, M13 9PL, UK

Virginia A. McNally, Mehdi Rajabi, Abdul Gbaj, Ian J. Stratford, Philip N. Edwards, Kenneth T. Douglas, Richard A. Bryce, Mohammed Jaffar, Sally Freeman

Morvus Technology Ltd, Building 115, Porton Down Science Park, Salisbury, SP4 OJQ, UK

Mohammed Jaffar

Correspondence: S. Freeman, School of Pharmacy and Pharmaceutical Sciences, University of Manchester, Oxford Road, Manchester, M13 9PL, UK. E-mail: sally.freeman@manchester.ac.uk

Acknowledgements and funding: We thank Oxford Biomedica (VAM), The Medical Research Council (IJS, MJ) and the Libyan Government (AG) for funding. We also thank Simon T. Barry and Richard W. A. Luke from AstraZeneca (Alderley Edge, UK) for providing the X-ray crystallographic co-ordinates of human TP.

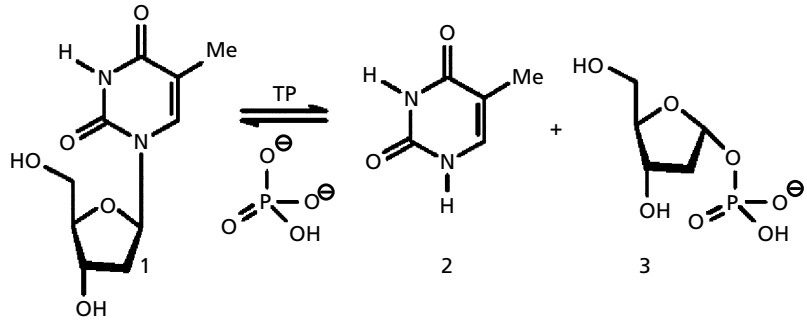

Figure 1 Phosphorolysis of thymidine (**1**) to thymine (**2**) and 2-deoxyribose-1-phosphate (**3**) by TP.

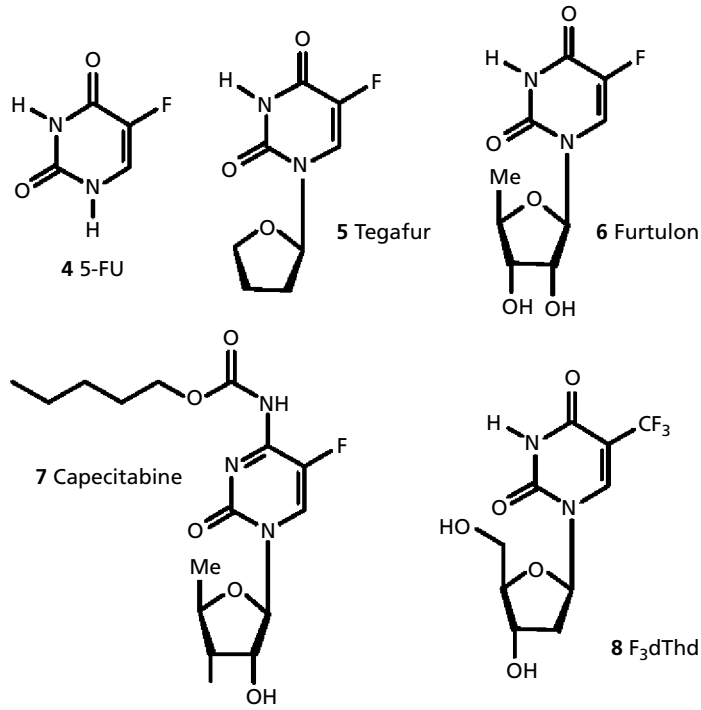

Figure 2 Fluoropyrimidine-based anti-cancer agents.

over-expressed human TP (Matsushita et al 1999). TP inhibitors (e.g., TPI) can also be used successfully in combination therapies with VEGF inhibitors to elicit an anti-angiogenic response (Relf et al 1997).

In recent years, a number of TP inhibitors have been synthesised (Figure 3). These include the 5- and 6-substituted uracil analogues (e.g., 6-amino-5-bromouracil (**10**, 6A5BU)) (Langen et al 1967; Pan et al 1998), multi-substrate alkylphosphonates (**11**, Y = alkyl chain) (Esteban-Gamboa et al 2000), transition-state analogues (Priego et al 2003) and the methylene-bridged bicyclic compounds of type **12** (Klein et al 2001; Murray et al 2002; Yano et al 2004a, b). Prodrugs of inhibitors of TP have also been synthesised in which 2-nitroimidazolyluracil prodrugs (**13**) require bioactivation under tumour conditions to form the active species, 2′-aminoimidazolyluracils (**14**) (Cole et al 2003; Reigan et al 2004, 2005). One compound in particular, 6-[(2′-aminoimidazol-1-yl)methyl]-5-bromouracil hydrochloride (IC50 (the concentration that inhibits the activity by 50%) 0.019 μM), was as potent an inhibitor of human TP as TPI (apparent IC50 0.023 μM) (Reigan et al 2004, 2005). In addition, inhibitors have been designed and synthesised with the aid of 3D-homology models of *Escherichia coli* and human TP (McNally et al 2003; Price et al 2003). Here we report the design of bicyclic ligands (similar in structure to TPI) using the X-ray crystal structure of human TP (Norman et al 2004) to predict inhibitors by exploring the binding modes and energetics of the ligands in the active site. We also describe the

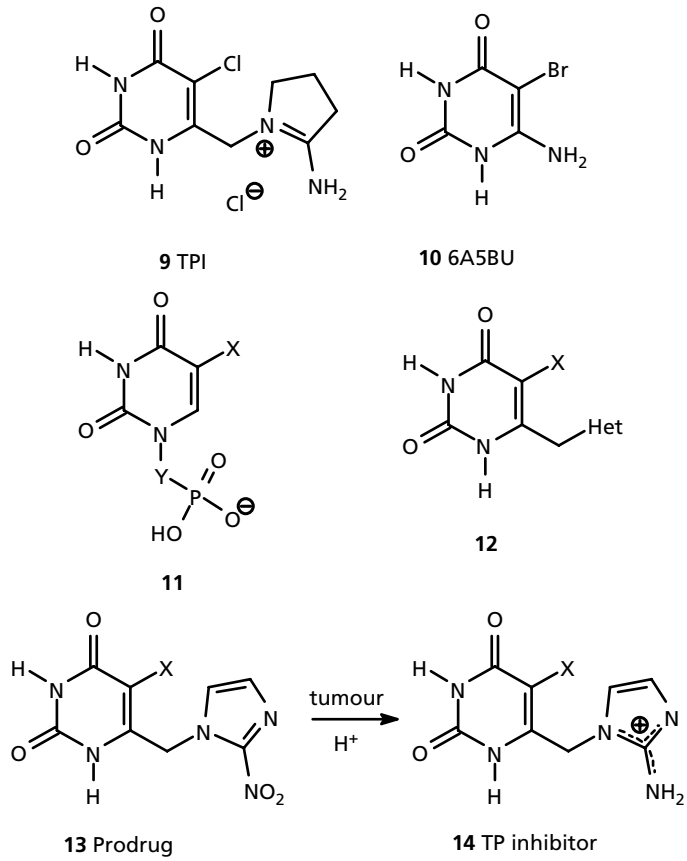

Figure 3 TP inhibitors.

synthesis of methylene-bridged and related conformationally restricted uracil-imidazolyl conjugates and report on the ability of the compounds synthesised to inhibit TP by using a multi-well enzymatic assay.

Materials and Methods

Materials

Nuclear magnetic resonance (NMR) spectra were recorded on a Jeol JNMR-EX270 270 MHz spectrometer or a Bruker Avance 300 MHz spectrometer. ^{1}H and ^{13}C NMR spectra are reported as δ_H parts per million (ppm) downfield from tetramethylsilane for samples run in $CDCl_3$ and DMSO-d_6. Benzene was used as an internal standard for ^{1}H and ^{13}C NMR samples dissolved in D_2O. ^{13}C NMR spectra were assigned with the aid of Distortionless Enhancement through Polarization Transfer (DEPT 135). Chemical peaks are indicated by: s (singlet), brs (broad singlet), d (doublet), dd (doublet of doublets), t (triplet), m (multiplet), q (quartet), p (pentet) and Ar (aromatic). Mass spectra were determined by the Chemistry Department, University of Manchester, using Micromass Trio 2000, chemical ionisation (CI), using NH_3 as an ionising gas. Electrospray (ES) mass spectra were recorded on a Micromass platform spectrometer using acetonitrile–water (1:1) as the mobile phase. Melting points were determined using a Gallenkamp MPD.350.BM2.5 instrument and remain uncorrected. Reactions were routinely monitored using thin-layer chromatography (TLC) on silica-gel plates (precoated F_{254}, Merck 1.05554) and spots were visualised using 254 nm UV light, $KMnO_4$ or DNP stain. Flash column chromatography was performed using Prolabo silica gel 60 (35–75 μm). Solvents for reactions were distilled from the indicated drying agents, following standard procedures. Chemicals were obtained from The Aldrich Chemical Co. (Dorset, UK) and Lancaster Synthesis Ltd. (Lancashire, UK). Human TP was a gift from AstraZeneca (UK).

Synthesis

5-Chloro-6-(chloromethyl)uracil (**18**)
Compound **18** was prepared from **17** and NCS as a colorless powder (89%) by a literature method (Murray et al 2002): mp 266–268°C. (Lit. (Johnson 1943) 270–275°C); ^{1}H NMR (270 MHz, DMSO-d_6) δ 4.46 (2H, s, C*H*$_2$Cl), 11.59 (1H, s, N*H*), 11.73 (1H, s, N*H*).

5-Bromo-6-(chloromethyl)uracil (**19**)
6-(Chloromethyl)uracil (**17**) (3.47 g, 21.70 mmol) was added to a mixture of glacial acetic acid (80 mL) and acetic anhydride (3 mL). The suspension was heated at 80°C under N_2

for 15 min. The suspension was cooled to 55°C and NBS (4.80 g, 27 mmol) was added. After stirring for 4 h at 55°C, the mixture was poured onto iced water (300 mL). The precipitate was collected, washed with water and dried to give **19** (3.35 g, 65%) as a colourless powder: mp > 260°C (dec.); ^{1}H NMR (270 MHz, DMSO-d_6) δ 4.47 (2H, s, CH_2Br); ^{13}C NMR (67.9 MHz, DMSO-d_6) δ 41.4 (*C*H$_2$Cl), 97.4 (*C*-5), 149.0 (*C*-6), 150.3 (*C*-2), 160.3 (*C*-4).

6-[(3-Methylimidazol-1-yl)methyl]uracil chloride (**15a**)

1-Methylimidazole (0.68 mL, 8.53 mmol) was added to a solution of 6-(chloromethyl)uracil (**17**) (0.46 g, 2.87 mmol) in methanol (MeOH, 10 mL). The mixture was heated at reflux for 16 h under N_2. The reaction was monitored by TLC (10% MeOH:DCM), which showed the presence of 6-(chloromethyl)uracil, and a further portion of 1-methylimidazole (0.3 mL, 3.76 mmol) was added. The mixture was heated at reflux for an additional 6 h. The reaction mixture was filtered under N_2 and washed with hot MeOH to give **15a** (0.50 g, 72%) as a colourless solid: mp 272–276°C; ^{1}H NMR (270 MHz, DMSO-d_6) δ 3.88 (3H, s, CH_3), 5.22 (2H, s, CH_2), 5.35 (1H, s, *H*-5), 7.76 (1H, s, *H*-4′ or *H*-5′), 7.82 (1H, s, *H*-4′ or *H*-5′), 9.24 (1H, s, *H*-2′), 11.20 (2H, brs, 2×N*H*); ^{13}C NMR (67.9 MHz, DMSO-d_6) δ 36.2 (*C*H$_3$), 48.3 (*C*H$_2$), 99.5 (*C*-5), 123.0 (*C*-4′), 124.2 (*C*-5′), 138.0 (*C*-6), 149.7 (*C*-2′), 151.5 (*C*-2), 164.0 (*C*-4); MS (ES+) 207 (M$^+$H, 100%), 413 (2M$^+$H, 13%, dimer); CHN: $C_9H_{11}ClN_4O_2$ expected: C 44.55, H 4.57, N 23.09%. Found: C 44.41, H 4.90, N 23.08%.

6-[(3-Methylimidazol-1-yl)methyl]thymine chloride (**15b**)

1-Methylimidazole (0.3 mL, 3.76 mmol) was added to a solution of 6-(chloromethyl)thymine (**21**) (0.20 g, 1.2 mmol) in chlorobenzene (3.5 mL). The mixture was heated at reflux for 16 h under N_2. The cooled suspension was filtered under N_2 and washed with hot MeOH to give **15b** (0.19 g, 62%) as a colourless solid: mp 282–283°C (dec.); ^{1}H NMR (270 MHz, DMSO-d_6) δ 1.87 (3H, s, CH_3), 3.86 (3H, s, N-CH_3), 5.20 (2H, s, CH_2), 7.75 (1H, d, $^3J_{HH}$ = 1.65 Hz, *H*-4′ or *H*-5′), 7.76 (1H, d, $^3J_{HH}$ = 1.65 Hz, *H*-4′ or *H*-5′), 9.17 (1H, s, *H*-2′), 10.94 (1H, brs, N*H*), 11.30 (1H, br, N*H*); ^{13}C NMR (67.9 MHz, DMSO-d_6) δ 9.45 (*C*H$_3$) 35.8 (N-*C*H$_3$), 46.5 (*C*H$_2$), 109.1 (*C*-5), 122.4 (*C*-4′), 123.8 (*C*-5′), 137.0 (*C*-6), 141.1 (*C*-2′), 150.5 (*C*-2), 164.6 (*C*-4); MS (ES+) 221 (M$^+$H, 100%).

5-Chloro-6-[(3-Methylimidazol-1-yl)methyl]uracil chloride (**15c**)

1-Methylimidazole (0.25 mL, 3.14 mmol) was added to a solution of 5-chloro-6-(chloromethyl)uracil (**18**) (0.41 g, 2.10 mmol) in chlorobenzene (10 mL). The mixture was heated at reflux for 19 h under N_2. The reaction mixture was filtered under N_2 and washed with hot MeOH to give **15c** (0.53 g, 92%) as a pale grey solid: mp > 310°C (dec.); ^{1}H NMR (270 MHz, DMSO-d_6) δ 3.88 (3H, s, CH_3), 5.36 (2H, s, CH_2), 7.77 (1H, d, $^3J_{HH}$ = 1.8 Hz, *H*-4′ or *H*-5′), 7.84 (1H, d, $^3J_{HH}$ = 1.8 Hz, *H*-4′ or *H*-5′), 9.26 (1H, s, *H*-2′), 11.79 (2H, brs, 2×N*H*); ^{13}C NMR (67.9 MHz, DMSO-d_6) δ 36.1 (*C*H$_3$), 46.9 (*C*H$_2$), 107.9 (*C*-5), 122.9 (*C*-4′), 124.1 (*C*-5′), 137.7 (*C*-6), 143.8 (*C*-2′), 150.0 (*C*-2), 159.9 (*C*-4); MS (ES+) 241 (M$^+$H, ^{35}Cl, 100%), 243 (M$^+$H, ^{37}Cl, 47%), 481 (2M$^+$H, ^{35}Cl, 15%, dimer), 483 (2M$^+$H, ^{37}Cl, 5%, dimer); CHN: $C_9H_{10}Cl_2N_4O_2$ expected: C 39.01, H 3.64, N 20.22%. Found: C 39.03, H 3.64, N 20.13%.

5-Bromo-6-[(3-Methylimidazol-1-yl)methyl]uracil chloride (**15d**)

1-Methylimidazole (0.17 mL, 2.13 mmol) was added to a solution of 5-bromo-6-(chloromethyl)uracil (**19**) (0.42 g, 1.75 mmol) in chlorobenzene (10 mL). The mixture was heated at reflux for 16 h under N_2. The reaction mixture was filtered under N_2 and washed with hot MeOH to give **15d** (0.42 g, 88%) as a pale grey solid: mp > 300°C (dec.); ^{1}H NMR (270 MHz, DMSO-d_6) δ 3.35 (3H, s, CH_3), 5.32 (2H, s, CH_2), 7.77 (1H, br d, *H*-4′ or *H*-5′), 7.81 (1H, br d, *H*-4′ or *H*-5′), 9.22 (1H, br d, *H*-2′), 11.66, (1H, brs, N*H*), 11.76 (1H, br, N*H*); ^{13}C NMR (67.9 MHz, DMSO-d_6) δ 36.1 (*C*H$_3$), 49.3 (*C*H$_2$), 98.6 (*C*-5), 122.9 (*C*-4′), 124.2 (*C*-5′), 137.6 (*C*-6), 145.4 (*C*-2′), 150.4 (*C*-2), 160.2 (*C*-4); MS (ES+) 285 (M$^+$H, ^{79}Br, 77%), 287 (M$^+$H, ^{81}Br, 100%); CHN: $C_9H_{10}BrClN_4O_2$ expected: C 33.62, H 3.13, N 17.42%. Found: C 33.56, H 2.94, N 17.15%.

6-Chlorouracil (**23**)

Compound **23** was prepared from 2,4,6-trichloropyrimidine (**22**) and NaOH as a colourless crystalline solid (83%) as previously described (Cresswell & Wood 1960): mp 306–308°C (Lit. (Marley & Plaut 1959) 301–302°C). ^{1}H NMR (300.1 MHz, DMSO-d_6) δ 5.75 (1H, s, *H*-5), 11.28 (1H, brs, N*H*), 12.04 (1H, brs, N*H*); ^{13}C NMR (75.5 MHz, DMSO-d_6) δ 100.2 (*C*-5), 145.1 (*C*-6), 150.7 (*C*-2), 163.0 (*C*-4); MS (ES-) 145 (M-H, ^{35}Cl, 100%), 147 (M-H, ^{37}Cl, 27%).

5,6-Dichlorouracil (**24**)

Compound **24** was prepared from 6-chlorouracil (**23**) and NCS as a pink solid (38%) as previously described (Murray et al 2002): mp 309–312°C (dec.) (Lit. (Berg-Nielsen et al 1972) 302–305°C); ^{1}H NMR (300.1 MHz, DMSO-d_6) δ 11.75 (2H, brs, 2×N*H*); ^{13}C NMR (75.5 MHz, DMSO-d_6) δ 105.7 (*C*-5), 142.7 (*C*-6), 149.2 (*C*-2), 159.2 (*C*-4); MS (ES-) 179 (M-H, ^{35,35}Cl, 100%), 181 (M-H, ^{35,37}Cl, 75%), 183 (M-H, ^{37,37}Cl, 2%).

5-Bromo-6-chlorouracil (**25**)

Compound **25** was prepared from 6-chlorouracil and Br_2 as a colourless solid (52%) using a literature procedure (Murray et al 2002): mp 298–300°C (dec.); ^{1}H-NMR (300.1 MHz, DMSO-d_6) δ 11.68 (2H, brs, 2×N*H*); ^{13}C NMR (75.5 MHz, DMSO-d_6) δ 95.5 (*C*-5), 144.4 (*C*-6), 149.2 (*C*-2), 159.2 (*C*-4); MS (ES-) 223 (M-H, ^{79}Br ^{35}Cl, 78%), 225 (M-H, ^{81}Br ^{35}Cl and ^{79}Br ^{37}Cl, 100%), 227 (M-H, ^{81}Br ^{37}Cl, 27%).

6-(3-Methylimidazol-1-yl)uracil chloride (**16a**)

1-Methylimidazole (0.18 mL, 2.26 mmol) was added to a solution of 6-chlorouracil (0.22 g, 1.50 mmol) in chlorobenzene (5 mL). The mixture was heated at reflux for 16 h under N_2. The cooled suspension was filtered under N_2 and washed

with hot MeOH to give **16a** (0.29 g, 84%) as a colourless solid: mp > 280°C (dec.); ^{1}H NMR (300.1 MHz, DMSO-d_6) δ 3.95 (3H, s, N-CH_3), 6.07 (1H, s, *H*-5), 7.95 (1H, t, $^3J_{HH} = {}^4J_{HH} = 1.8$ Hz, *H*-4′ or *H*-5′), 8.19 (1H, t, $^3J_{HH} = {}^4J_{HH} = 1.8$ Hz, *H*-4′ or *H*-5′), 9.84 (1H, brs, *H*-2′), 11.45 (1H, brs, N*H*), (1H, brs, N*H*); ^{13}C NMR (75.5 MHz, DMSO-d_6) δ 36.4 (N-*C*H_3′), 93.1 (*C*-5), 120.6 (*C*-4′ or *C*-5′), 124.2 (*C*-4′ or *C*-5′), 137.1 (*C*-2′), 144.4 (*C*-6), 150.9 (*C*-2), 163.8 (*C*-4); MS (ES+) 193 (M^+H, 75%), 385 ($2M^+$H, 100%, dimer); CHN: $C_8H_9ClN_4O_2$ expected: C 42.03, H 3.97, N 24.50%. Found: C 41.93, H 4.00, N 24.37%.

5-Chloro-6-(3′-methylimidazol-1-yl)uracil chloride (**16c**)

Compound **16c** was prepared from 5,6-dichlorouracil (**25**) and 1-methylimidazole using the method described for **16a**. The product was isolated as a colourless powder (56%): mp 276–278°C (dec.); ^{1}H NMR (300.1 MHz, DMSO-d_6) δ 3.95 (3H, s, N-CH_3), 7.81 (1H, t,$^3J_{HH} = {}^4J_{HH} = 1.9$ Hz, *H*-4′ or *H*-5′), 8.11 (1H, t, $^3J_{HH} = {}^4J_{HH} = 1.9$ Hz, *H*-4′ or *H*-5′), 9.65 (1H, brs, *H*-2′), 10.41 (2H, brs, N*H*); ^{13}C NMR (75.5 MHz, DMSO-d_6) δ 36.1 (N-*C*H_3′), 91.4 (*C*-5), 121.7 (*C*-4′ or *C*-5′), 122.9 (*C*-4′ or *C*-5′), 136.9 (*C*-2′), 150.6 (*C*-6), 155.9 (*C*-2), 162.3 (*C*-4); MS (ES+) 227 (M^+H, ^{35}Cl, 100%), 229 (M^+H, ^{37}Cl, 30%), 453 ($2M^+$H, ^{35}Cl, 20%, dimer), 455 ($2M^+$H, ^{37}Cl, 7%, dimer); CHN: $C_8H_8Cl_2N_4O_2$ expected: C 36.52, H 3.07, N 21.03%. Found: C 36.83, H 3.42, N 21.56%.

5-Bromo-6-(3′-methylimidazol-1-yl)uracil chloride (**16d)**

Compound **16d** was prepared from 5-bromo-6-chlorouracil (**27**) and 1-methylimidazole using the method described for **16a** as a colourless powder (77%): mp 268–270°C (dec.); ^{1}H NMR (300.1 MHz, DMSO-d_6) δ 3.94 (3H, s, N-CH_3), 7.81 (1H, t, $^3J_{HH} = {}^4J_{HH} = 1.9$ Hz, *H*-4′ or *H*-5′), 8.11 (1H, t, $^3J_{HH} = {}^4J_{HH} = 1.8$ Hz, *H*-4′ or *H*-5′), 9.64 (1H, brs, *H*-2′), 10.40 (1H, brs, N*H*), 11.20 (1H, brs, N*H*); ^{13}C NMR (75.5 MHz, DMSO-d_6) δ 36.2 (N-*C*H_3′), 91.9 (*C*-5), 121.8 (*C*-4′ or *C*-5′), 123.1 (*C*-4′ or *C*-5′), 137.0 (*C*-2′), 144.3 (*C*-6), 155.7 (*C*-2), 162.2 (*C*-4); CHN: $C_8H_8BrClN_4O_2$ expected: C 31.24, H 2.62, N 18.22%. Found: C 31.70, H 3.00, N 18.80%.

Thymidine phosphorylase inhibition assay

Enzyme rate spectral scans, studies of inhibition curves and absorbance readings at fixed wavelengths were conducted using a Peltier-thermostatted cuvette holder in a Cary 4000 UV-visible spectrophotometer and Cary Enzyme Kinetics Software. The assay contained in 1 mL 20 μM thymidine, 0.1 M potassium phosphate (pH 7.4), and limiting amounts of human TP (0.22 U) (gift from AstraZeneca). The reaction was initiated by addition of enzyme and the change in absorbance was monitored at 265 nm at 25°C (Nakayama et al 1980; Reigan et al 2005). The IC50 values were generated by fitting each inhibition data set to the competitive inhibition equation by non-linear regression analysis (GraFit version 3.0; Erithacus Software Ltd, UK). All IC50 measurements were performed in duplicate or triplicate.

Statistical methods

Statistical analysis of the inhibition data were performed using a one-way analysis of variance (http://web.umr.edu/~psyworld/tukeyssteps.htm) using 8 different concentrations of the inhibitor for at least two independent experiments. In all cases, post-hoc comparisons of the means of individual groups were performed using Tukey's Honestly Significant Difference Test. $P < 0.05$ ($F = 3.49$) denoted significance in all cases.

Molecular modelling

Docking studies employed the X-ray crystal structure of human thymidine phosphorylase in complex with the inhibitor TPI and in the absence of phosphate (resolution 2.11 Å, PDB code 1UOU) (Norman et al 2004). The location of hydrogen atoms were modelled into the structure using SYBYL 6 (Tripos Inc.); location of the active site phosphate molecule was performed via analogy with the crystal structure of *B. stearothermophilus* pyrimidine nucleoside phosphorylase (PyNP) where the phosphate group is present (Pugmire & Ealick 1998). Three-dimensional structures of the designed ligands **15a–d** and **16a–d** were assigned using ViewerLite (Accelrys Software Inc.). For computational docking using the program DOCK 4 (Ewing et al 2001), the protein was assigned Gasteiger-Marsili atom-centred partial point charges (Gasteiger & Marsili 1980); treating the uracil moieties as 2-oxy-anion-3,4-dihydro-4-oxopyrimidine, the ligands were assigned charges consistent with the MMFF94s force field (Halgren 1996). Ligands were docked flexibly into the active site of TP, using an anchor-first search with automated matching; 500 orientations and 25 (pruned) configurations per cycle were considered. Energy minimisation was performed for 500 iterations, using a distance-dependent dielectric of 1.5r.

Results and Discussion

Inhibitor design and molecular modelling

The chemical features of TPI and aminouracil analogues of **10** were used as a starting point for structural design due to their ability to inhibit human TP. Based on initial observations of the active site and its interactions with TPI, imidazoyl-bridged uracil analogue series **15** and **16** were proposed as putative TP inhibitors (Figure 4).

The computational docking of TPI and ligands **15** and **16** into the active site of TP was considered. In-silico docking of TPI to the protein reproduced the crystallographically observed binding mode (Table 1, Figure 5): the nucleotide base interacted via hydrogen bonds with residues Ser217, Arg202, Lys221 and His116; the substituent at position 5 projected into a lipophilic pocket formed by residues Leu148, Val208, Ile214 and Val241; the NH_2 group of the iminopyrrolidine ring interacted with an oxygen atom of the bound phosphate group (O···H-N distance of 2.9 Å). Compounds **15a–d** were predicted to bind in an analogous orientation to TPI in the active site, with the uracil moiety

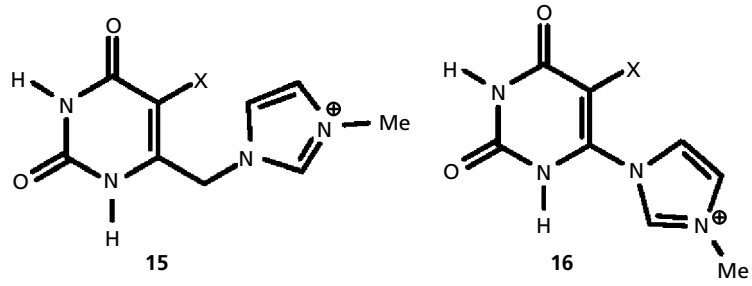

Figure 4 Designed ligands as potential TP inhibitors.

Table 1 The predicted binding modes of ligand series **15** and **16** in active site of TP. Selected inter-atomic distances in Å

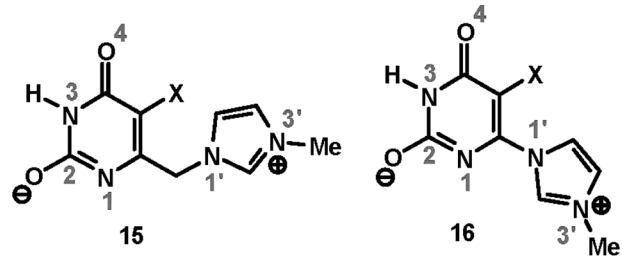

Compound	X	Polar distances (Å)		Apolar distances (Å)
15a	H	O4–H-N$\eta^{1/2}$Arg202 (2.5,2.2) N1–H-Nε His116 (2.1) O2–H-NεHis116 (2.3)	O2–H-Nζ Lys221 (2.3) N3-H–Oγ Ser217 (1.9)	H–H-Cδ Ile 214 (2.3)
15b	Me	O4–H-N$\eta^{1/2}$Arg202 (2.2. 2.2) N3-H–Oγ Ser217 (1.8) O2–H-Nζ Lys221 (2.0)	O2–H-NεHis116 (2.1) N1–H-NεHis116 (2.0)	
15c	Cl	O4–H-N$\eta^{1/2}$Arg202 (1.9, 2.1) N3-H–Oγ Ser217 (2.1) N1–H-Nε His116 (2.0)	O2–H-Nζ Lys221 (2.3) O2–H-Nε His116 (2.3)	Cl–H-Cγ^1Val241 (2.9) Cl–H-Cδ^1Leu148 (2.7)
15d	Br	O4–H-Nη^2Arg202 (2.4) N3-H–Oγ Ser217 (2.1) O2–H-NζLys221 (2.3)	O2–H-NεHis116 (2.2) N1–H-NεHis116 (1.9)	Br–H-Cγ^1Val241 (2.7) Br–H-Cδ^1Leu148 (3.0) Br–H-Cδ Ile214 (3.2)
16a	H	N3-H–Oγ Ser217 (4.6) N1–H-NεHis116 (2.2)	O2–H-NεHis116 (2.5) N3′–O1-P(3.1)	
16b	Me	N3-H–Oγ Ser217 (2.5) O2–H-Nζ Lys221 (2.0, 2.7) N1–H-NεHis116 (2.4)	O4–Nη^2Arg202 (3.1) N3′–O1-P (7.4)	
16c	Cl	O4–H-N$\eta^{1/2}$Arg202 (2.2, 2.3) N3-H–Oγ Ser217 (2.7) O2–H-NζLys221 (2.1)	O2–H-NεHis116 (2.2) N1–H-NεHis116 (2.7)	Cl–H-CδIle214 (2.5) Cl–H-Cδ^1Leu148 (2.7)
16d	Br	O4–H-NεArg202 (2.2) N3-H–Oγ Ser217 (2.3)	O2–H-Nζ Lys221 (2.3) N1–H-NεHis116 (2.6)	Br–H-Cγ^1Val241 (2.6) Br–H-Cδ^1Leu148 (2.7)
TPI	—	O4–H-N$\eta^{1/2}$ Arg202 (1.9, 2.4) N3-H–OγSer217 (2.1) O2–H-Nζ Lys221 (2.1)	O2–H-Nε^2His116 (2.2) N1–H-Nε^2His116 (2.0) N2–O1-P (2.9)	Cl–H-Cδ^1Leu148 (2.5) Cl–H-Cγ^1Val241 (2.9)

occupying the nucleoside binding pocket (e.g., compound **15c** in Figure 5); similar inter-atomic distances to polar and apolar residues were observed (Table 1). The imidazoyl ring did not have a pendant NH_2 group; instead, in each of compounds **15a–d**, the N-methyl motif projected away from the phosphate, forming contacts with hydrophobic residues (Leu148 and Val241).

The computationally predicted binding modes of compounds **16** (without a methylene group between the uracil and imidazoyl rings) were also considered. Relative to the binding modes of TPI and **15**, compounds **16a–d** appeared displaced towards the centre of the active site region (Table 1). Interactions with the nucleoside binding pocket were still formed, although a key interaction between N1 and H-N of

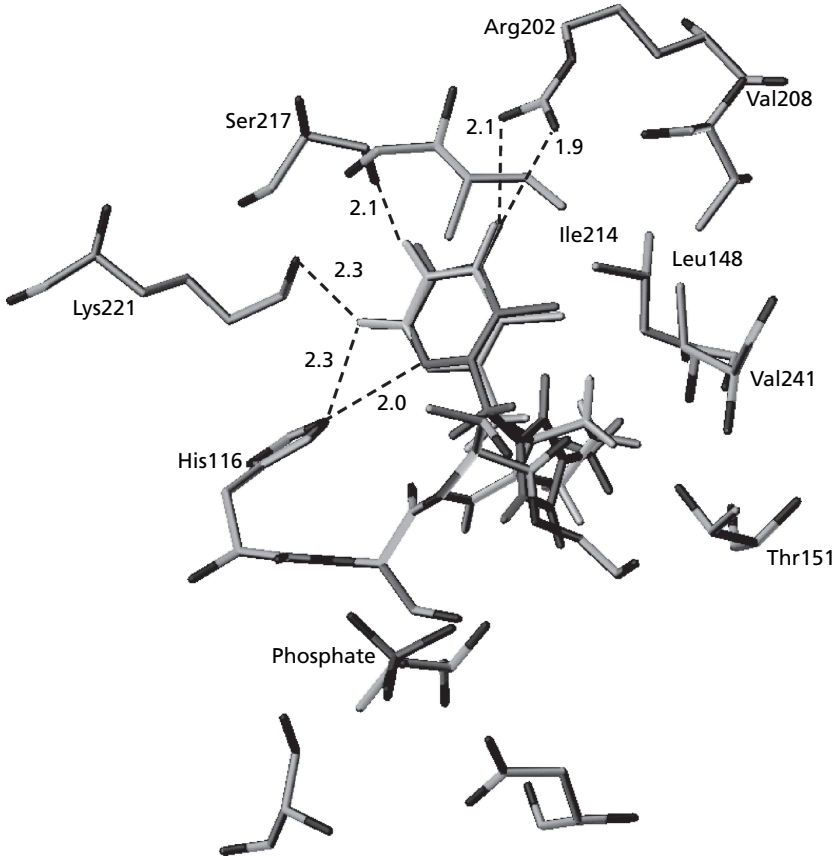

Figure 5 Predicted binding mode of TPI (light) and compound **15c** (dark) in active site of human TP. Selected inter-atomic distances between **15c** and TP are shown (Å).

His116 was weakened, with for example a distance of 2.7 Å in compound **16c** (Table 1, Figure 6) compared with 2.0 Å in the corresponding methylene-bridged ligand **15c**. Similarly, the N3-H $\cdots$ Oγ of Ser217 distance was lengthened from 2.1 Å to 2.7 Å. For compound **16a**, this effect was more pronounced, with an increase in the N3-H$\cdots$Oγ of Ser217 distance from 1.9 Å to 4.6 Å on removal of the methylene group (Table 1). The docked conformations of compounds **16** also appeared tilted with respect to TPI and **15**—a consequence of steric constraints arising from inflexibility due to the absent bridging CH_2 group. These constraints centered around proximity of the imidazoyl group to residues Ser117, Gly119 and Thr151 (Figure 6), and may also have contributed to the predicted orientation of the N-methyl group of **16** towards the phosphate, in contrast to **15**.

Consequently, computational docking suggested that compounds **15** interacted more completely than **16** with the active site residues of TP. While recognising the limitations of scoring functions used in docking to predict binding energies (relative to their good success with ligand–protein geometries), the preference of TP for **15** over **16** was reflected in the calculated binding affinity: the average interaction energy for compounds **16** was 4.2 kcal mol^{-1} less favourable than for compounds **15** and 19.8 kcal mol^{-1} less than for TPI. Although indicative, quantitative prediction of relative binding affinity here would require estimates of contributions from solvation, entropy and other factors, attainable through computationally costly thermodynamic perturbation calculations.

Chemical synthesis

The syntheses of the 5-substituted-6-methylimidazolyluracil analogues (**15a–d**) were achieved as illustrated in Figure 7 (Murray et al 2002; Yano et al 2004a, b). Treatment of the commercially available 6-chloromethyluracil (**17**) with NCS or NBS in glacial acetic acid for 15 h at elevated temperatures gave the 5-chloro- (**18**) and 5-bromo (**19**) derivatives in good yields (89% and 65%, respectively). Heating **18** or **19** with 1-methylimidazole in toluene for 16 h under N_2 gave the desired target compounds **15c** (92%) and **15d** (88%) in excellent yields. Reaction of **17** with 1-methylimidazole in MeOH for 16 h under N_2 gave the 5-unsubstituted analogue (**15a**) in 72% yield. The synthesis of the intermediate, 6-chloromethylthymine (**21**), was achieved in 3 steps from **20** as described by Murray et al (2002). Similarly, addition of 1-methylimidazole with **21** heated at reflux with chlorobenzene gave the 6-methyl target compound **15b** in 62% yield.

The conformationally-restricted 5-halogenated analogues (**16c** and **16d**) were synthesised in 3 steps from commercially available 2,4,6-trichloropyrimidine (**22**) (Niemz et al 1997). Briefly, **22** was treated with NaOH to give 6-chlorouracil

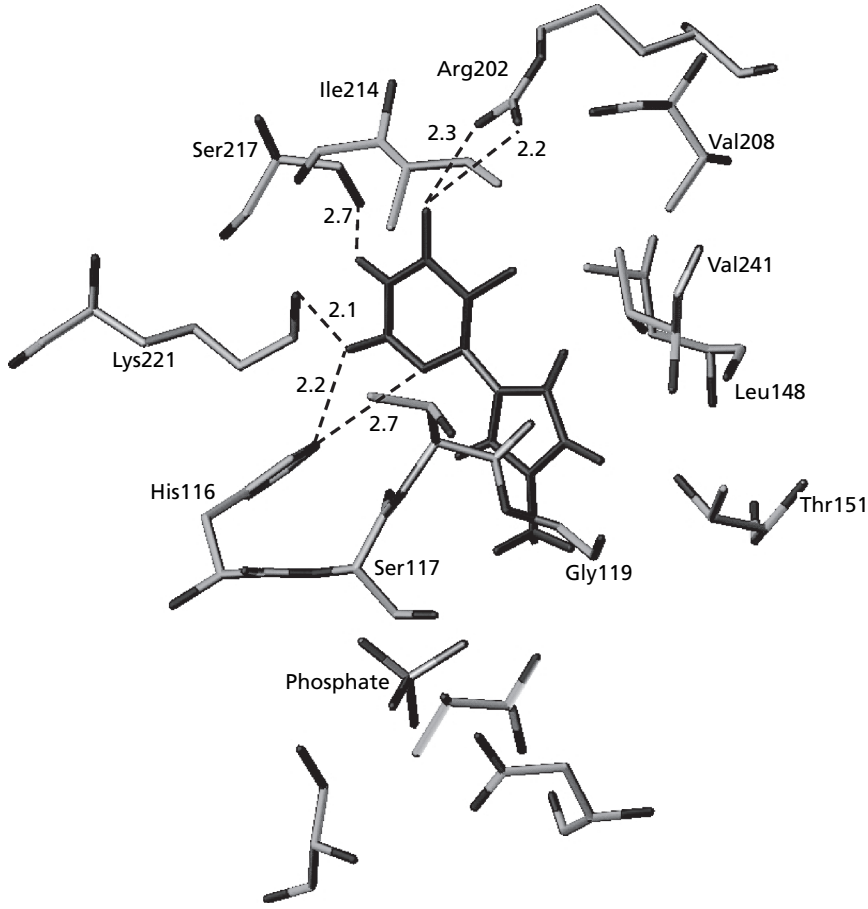

Figure 6 In-silico docked binding mode of compound **16c** in active site of human TP. Selected inter-atomic distances between **16c** and TP are shown (Å).

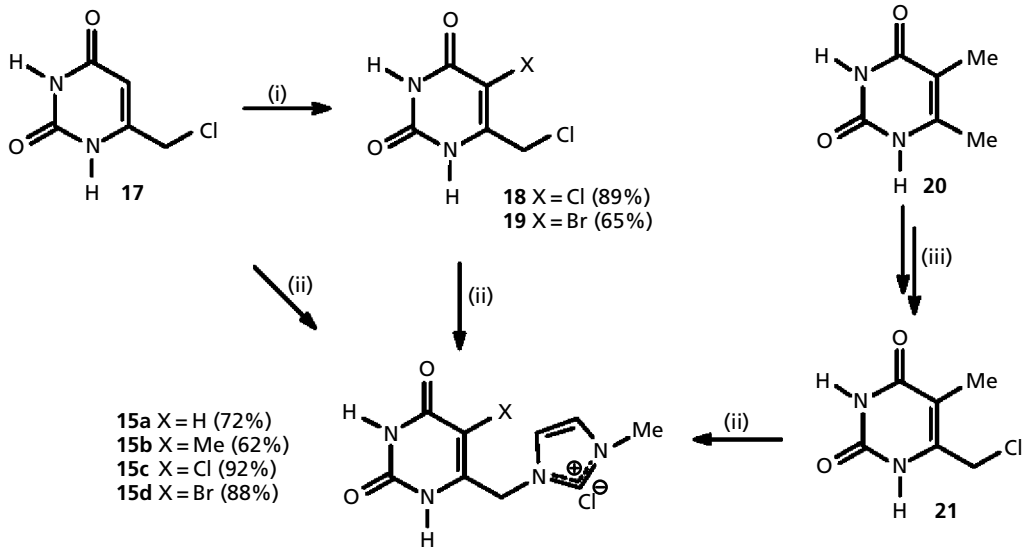

Figure 7 Synthesis of 6-methylimidazolylluracil derivatives (**15a–d**). Reagents and conditions: (i) AcOH, Ac_2O, NCS or NBS, Δ, N_2; (ii) 1-methylimidazole, Δ, N_2; (iii) Murray et al (2002).

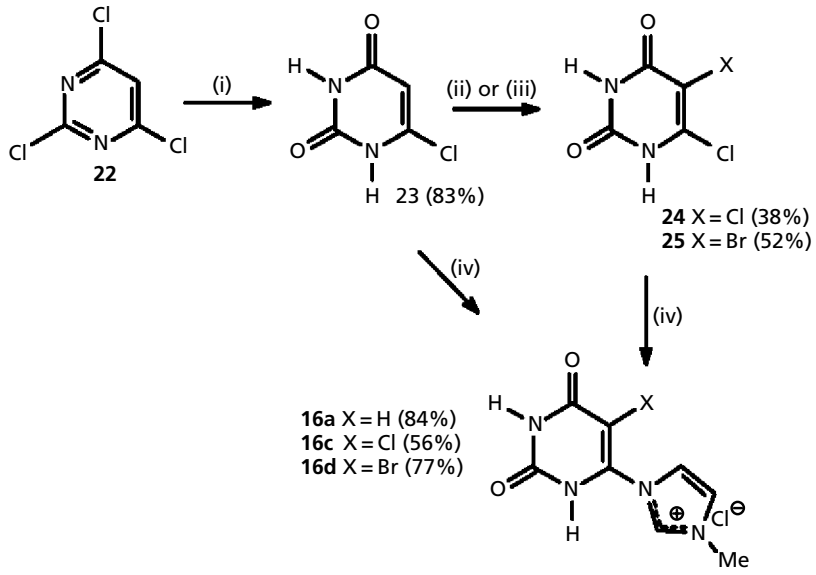

Figure 8 Synthesis of 6-imidazolyluracil analogues (**16a, c** and **d**). Reagents and conditions: (i) NaOH, 16 h, (ii) AcOH, Ac_2O, NCS, Δ, N_2; (iii) H_2O, Br_2, Δ; (iv) 1-methylimidazole, PhCl, 16 h, Δ, N_2.

(**23**). Reaction of **23** with NCS or Br_2 with heating at reflux gave the 6-halo-5-chlorouracil derivatives **24** and **25**, respectively. Conjugation of **24** and **25** with 1-methylimidazole at the C-6 position by heating at reflux for 16 h in chlorobenzene gave the desired compounds **16c** and **16d**. Direct coupling of 6-chlorouracil (**23**) with 1-methylimidazole gave the 5-unsubstituted analogue **16a** (Figure 8).

TP inhibition

All the compounds were tested for their TP inhibitory activity using recombinant human TP. A spectrophotometric assay was used to measure the decrease in absorbance (at 265 nm) of the natural substrate thymidine when the compounds were added (Nakayama et al 1980; Reigan et al 2004). The experimental IC50 values (the concentration of compound that inhibits the activity by 50%) are presented in Table 2. The compounds were compared with the known inhibitor TPI.

The inhibition data suggest that an electron-withdrawing substituent at the C-5 position of the uracil ring results in an increase in inhibition (Cole et al 2003; Reigan et al 2004). For instance, in the methylene-bridged series, **15d** (X = Br) is approximately 2.5-fold more potent as an inhibitor than **15a** (X = H). Similarly, in the conformationally-restricted conjugate series, **16d** (X = Br) is 3-fold more potent than **16a** (X = H). This observation is consistent with previous studies, which suggested that the improved active site–ligand interaction is due to the 5-halo group being situated in a lipophilic pocket of the enzyme (McNally et al 2003; Reigan et al 2005). Alternatively, it may be attributed to the increased acidity of the N1 for the halo derivatives (**15c, 15d, 16c, 16d**), with the zwitterionic resonance, being bound to TP (as seen in Table 1). However, the synthesised compounds showed much reduced inhibition as compared with TPI, which could be attributed to many reasons. Firstly, the enhanced activity of TPI may be due to some extra flexibility of the iminopyrrolidinyl ring (as compared with the planar imidazolyl ring in **15** and **16**). Secondly, TPI has a (protonated) amino group on C2′, appropriately positioned to hydrogen bond with a water pocket associated with phosphate, in contrast to **15** and **16** whose positive charge is too far away from the water pocket. Thirdly, the NH in TPI has a more appropriate pK_a value to give an anion on O(4) (Reigan et al 2005), resulting in a better

Table 2 Inhibition of the methylimidazole uracil analogues **15** and **16** with human TP, and their pK_a data

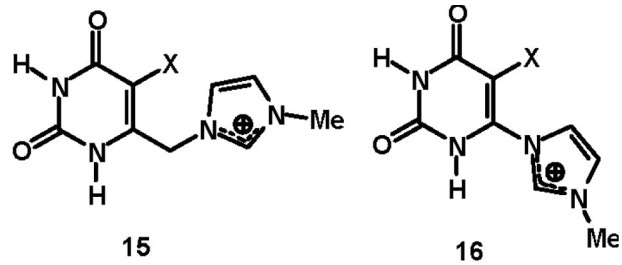

Compound	X	IC50 (μM)[a]	pK_a (A270)[b]
15a	H	42 ± 5.5	—[c]
15b	Me	60 ± 5.0	7.57 ± 0.06
15c	Cl	18 ± 2.0	—[c]
15d	Br	17 ± 2.0	5.57 ± 0.04
16a	H	110 ± 8.0	—[c]
16c	Cl	35 ± 4.0	1.26 ± 0.10
16d	Br	38 ± 3.0	1.30 ± 0.10
TPI	—	0.034 ± 0.03	6.1[d]

[a]$P < 0.05$ Tukey's HSD test. [b]Measured by UV spectroscopy at 25°C. [c]Not determined. [d]Reigan et al (2005).

mimic of the oxocarbenium transition state with tighter binding to the active site (Gbaj et al 2006).

Conclusions

The methylene-bridged series (**15**) were more potent inhibitors than the non-bridged series (**16**), which may be due, in part, to the more appropriate pK_a values of N1 and N3 for the methylene-bridged derivatives. This observation had been discussed by Reigan et al (2005), suggesting that strong acids, such as **16c** and **16d**, may result in poor binding to active site residues (e.g. Ser217) contributing to a decrease in IC50 values. The most potent inhibitor was **15d** with an IC50 of 17 μM. Overall, this study suggests that the active site of human TP is quite flexible and this revised model, which now includes the phosphate group, can be used for designing other inhibitors of TP.

References

Berg-Nielsen, K., Stensrud, T., Bernatek, E. (1972) Heterocyclics from malonyl chlorides. 3. Cyclization and oxidation of some 2-alkylthiopyrimidones. *Acta Chem. Scand*. **26**: 947–951

Brown, N. S., Bicknell, R. (1998) Thymidine phosphorylase, 2-deoxy-D-ribose and angiogenesis. *Biochem. J*. **334**: 1–8

Cole, C., Reigan, P., Gbaj, A., Edwards, P. N., Douglas, K. T., Stratford, I. J., Freeman, S., Jaffar, M. (2003) Potential tumor-selective nitroimidazolylmethyluracil prodrug derivatives: inhibitors of the angiogenic enzyme thymidine phosphorylase. *J. Med. Chem*. **46**: 207–209

Cresswell, R. M., Wood, H. C. S. (1960) The biosynthesis of pteridines. 1. The synthesis of riboflavin. *J. Chem. Soc*. 4768–4775

Esteban-Gamboa, A., Balzarini, J., Esnouf, R., De Clercq, E., Camarasa, M. J., Perez Perez, M. J. (2000) Design, synthesis, and enzymatic evaluation of multisubstrate analogue inhibitors of *Escherichia coli* thymidine phosphorylase. *J. Med. Chem*. **43**: 971–983

Ewing T. J. A., Makino S., Skillman A. G., Kuntz I. D. (2001) DOCK 4.0: search strategies for automated molecular docking of flexible molecule databases. *J. Comput.-Aided Mol. Des*. **15**: 411–428

Fukushima, M., Suzuki, N., Emura, T., Yano, S., Kazuno, H., Tada, Y., Yamada, Y., Asao, T. (2000) Structure and activity of specific inhibitors of thymidine phosphorylase to potentiate the function of antitumor 2′-deoxyribonucleosides. *Biochem. Pharmacol*. **59**: 1227–1236

Gasteiger, J, Marsili, M. (1980) Iterative partial equalization of orbital electronegativity – a rapid access to atomic charges. *Tetrahedron* **36**: 3219–3288

Gbaj, A., Edwards, P. N., Reigan, P., Freeman, S., Jaffar, M., Douglas, K. T. (2006) Thymidine phosphorylase from *Escherichi coli*: tight-binding inhibitors as enzyme active-site titrants. *J. Enyzme Inhib. Med. Chem*. **21**: 69–73

Griffiths, L., Stratford, I. J. (1997) Platelet-derived endothelial cell growth factor thymidine phosphorylase in tumour growth and response to therapy. *Br. J. Cancer* **76**: 689–693

Griffiths, L., Stratford, I. J. (1998) The influence of elevated levels of platelet-derived endothelial cell growth factor/thymidine phosphorylase on tumourigenicity, tumour growth, and oxygenation. *Int. J. Rad. Oncol. Biol. Phys*. **42**: 877–883

Halgren, T. A. (1996) Merck molecular force field. I. Basis, form, scope, parameterization, and performance of MMFF94. *J. Comput. Chem*. **17**: 490–512

Ishikawa, T., Sekiguchi, F., Fukase, Y., Sawada, N., Ishitsuka, H. (1998) Positive correlation between the efficacy of capecitabine and doxifluridine and the ratio of thymidine phosphorylase to dihydropyrimidine dehydrogenase activities in tumors in human cancer xenografts. *Cancer Res*. **58**: 685–690

Johnson, T. B. (1943) The reaction of hydrochloric acid with 6-methyl-5,5 dichloroxyhydrouracil. *J. Am. Chem. Soc*. **65**: 1220–1222

Klein, R. S., Lenzi, M., Lim, T. H., Hotchkiss, K. A., Wilson, P., Schwartz, E. L. (2001) Novel 6-substituted uracil analogs as inhibitors of the angiogenic actions of thymidine phosphorylase. *Biochem. Pharmacol*. **62**: 1257–1263

Kono, A, Hara, Y, Matsushima, Y. (1981) Enzymatic formation of 5-fluorouracil from 1-(tetrahydro-2-furanyl)-5-fluorouracil (Tegafur) in human-tumor tissues. *Chem. Pharm. Bull*. **29**: 1486–1488

Kono, A., Hara, Y., Sugata, S., Karube, Y., Matsushima, Y., Ishitsuka H. (1983) Activation of 5′-deoxy-5-fluorouridine by thymidine phosphorylase in human tumors. *Chem. Pharm. Bull*. **31**: 175–178

Krenitsky, T. A., Koszalka, G. W., Tuttle, J. V. (1981) Purine nucleoside synthesis: an efficient method employing nucleoside phosphorylases. *Biochemistry* **20**: 3615–3621

Langen, P., Etzold, G., Barwolff, D., Preussel, B. (1967) Inhibition of thymidine phosphorylase by 6-aminothymine and derivatives of 6-aminouracil. *Biochem. Pharmacol*. **16**: 1833–1837

Maeda, K., Kang, S. M., Ogawa, M., Onoda, N., Sawada, T., Nakata, B., Kato, Y., Chung, Y. S., Sowa, M. (1997) Combined analysis of vascular endothelial growth factor and platelet-derived endothelial cell growth factor expression in gastric carcinoma. *Int. J. Cancer* **74**: 545–550

Marley, G. F., Plaut, G. W. E. (1959) The isolation, synthesis, and metabolic properties of 6,7-dimethyl-8-ribityllumazine. *J. Biol. Chem*. **234**: 641–647

Matsushita, S., Nitanda, T., Furukawa, T., Sumizawa, T., Tani, A., Nishimoto, K., Akiba, S., Miyadera, K., Fukushima, M., Yamada, Y., Kanuki, T., Akiyame, S. (1999) The effect of a thymidine phosphorylase inhibitor on angiogenesis and apoptosis in tumors. *Cancer Res*. **59**: 1911–1916

McNally, V. A., Gbaj, A., Douglas, K. T., Stratford, I. J., Jaffar, M., Freeman, S., Bryce, R. A. (2003) Identification of a novel class of inhibitor of human and *Escherichia coli* thymidine phosphorylase by in silico screening. *Bioorg. Med. Chem. Lett*. **13**: 3705–3709

Miwa, M., Cook, A., Ishitsuka, H. (1986) Enzymatic cleavage of various fluorinated pyrimidine nucleosides to 5-fluorouracil and their antiproliferative activities in human and murine tumor-cells. *Chem. Pharm. Bull*. **34**: 4225–4232

Murray, P. E., McNally, V. A., Lockyer, S. D., Williams, K. J., Stratford, I. J., Jaffar, M., Freeman, S. (2002) Synthesis and enzymatic evaluation of pyridinium substituted uracil derivatives as novel inhibitors of thymidine phosphorylase. *Bioorg. Med. Chem*. **10**: 525–530

Nakayama, C., Wataya, Y., Meyer, R. B., Santi, D. V., Saneyoshi, M., Ueda, T. (1980) Thymidine phosphorylase. Substrate specificity for 5-substituted-2′-deoxyuridines. *J. Med. Chem*. **23**: 962–964

Niemz, A., Imbriglio, J., Rotello, V. M. (1997) Model systems for flavoenzyme activity: one- and two-electron reduction of flavins in aprotic hydrophobic environments. *J. Am. Chem. Soc*. **119**: 887–892

Norman, R. A., Barry, S. T., Bate, M., Breed, J., Colls, J. G., Ernill, R. J., Luke, R. W. A., Minshull, C. A., McAlister, M. S. B., McCall, E. J., McMiken, H. H. J., Paterson, D. S., Timms, D., Tucker, J. A., Pauptit, R. A. (2004) Crystal structure of human thymidine phosphorylase in complex with a small molecule inhibitor. *Structure* **12**: 75–84

O'Brien, T. S., Fox, S. B., Dickinson, A. J., Turley, H., Westwood, M., Moghaddam, A., Gatter, K. C., Bicknell, R., Harris, A. L. (1996) Expression of the angiogenic factor thymidine phosphorylase/platelet-derived endothelial cell growth factor in primary bladder cancers. *Cancer Res*. **56**: 4799–4804

Pan, B. C., Chen, Z. H., Chu, E., Chu, M. Y. W., Chu, S. H. (1998) Synthesis of 5-halogeno-6-amino-2′-deoxyuridines and their analogs as potential inhibitors of thymidine phosphorylase. *Nucleosides Nucleotides* **17**: 2367–2382

Patterson, A. V., Zhang, H., Moghaddam, A., Bicknell, R., Talbot, C. D., Stratford, I. J., Harris, A. L. (1995) Increased sensitivity to the prodrug 5′-deoxy-5 fluorouridine with modulation of 5-fluoro-2′-deoxyuridine sensitivity in MCF-7 cells transfected with thymidine phosphorylase. *Br. J Cancer* **72**: 669–675

Price, M. L. P., Guida, W. C., Jackson, T. E., Nydick, J. A., Gladstone, P. L., Juarez, J. C., Donate, F., Ternansky, R. J. (2003) Design of novel N-(2,4-dioxo-1,2,3,4 tetrahydro-thieno[3,2-d]pyrimidin-7-yl)-guanidines as thymidine phosphorylase inhibitors, and flexible docking to a homology model. *Bioorg. Med. Chem. Lett*. **13**: 107–110

Priego, E. M., Mendieta, J., Gago, F., Balzarini, J., De Clercq, E., Camarasa, M. J., Perez-Perez, M. J. (2003) Towards new thymidine phosphorylase/PD-ECGF inhibitors based on the transition state of the enzyme reaction. *Nucleosides Nucleotides Nucleic Acids* **22**: 951–953

Pugmire, M. J., Ealick S. E. (1998) The crystal structure of pyrimidine nucleoside phosphorylase in a closed conformation. *Structure* **6**: 1467–1479

Reigan, P., Gbaj, A., Chinje, E., Stratford, I. J., Douglas, K. T., Freeman, S. (2004) Synthesis and enzymatic evaluation of xanthine oxidase-activated prodrugs based on inhibitors of thymidine phosphorylase. *Bioorg. Med. Chem. Lett* **14**: 5247–5250

Reigan, P., Edwards, P. N., Gbaj, A., Cole, C., Barry, S. T., Page, K. M., Ashton, S. E., Luke, R. W. A., Douglas, K. T., Stratford, I. J., Jaffar, M., Bryce, R. A., Freeman, S. (2005) Aminoimidazolylmethyluracil analogues as potent inhibitors of thymidine phosphorylase and their bioreductive nitroimidazolyl prodrugs. *J. Med. Chem*. **48**: 392–402

Relf, M., LeJeune, S., Scott, P. A. E., Fox, S., Smith, K., Leek, R., Moghaddam, A., Whitehouse, R., Bicknell, R., Harris, A. L. (1997) Expression of the angiogenic factors vascular endothelial cell growth factor, acidic and basic fibroblast growth factor, tumor growth factor beta-1, platelet-derived endothelial cell growth factor, placenta growth factor, and pleiotrophin in human primary breast cancer and its relation to angiogenesis. *Cancer Res*. **57**: 963–969

Reynolds, K., Farzaneh, F., Collins, W. P., Campbell, S., Bourne, T. H., Lawton, F., Moghaddam, A., Harris, A. L., Bicknell, R. (1994) Association of ovarian malignancy with expression of platelet-derived endothelial-cell growth factor. *J. Natl. Cancer Inst*. **86**: 1234–1238

Schwartz, E. L., Baptiste, N, O'Connor, C. J., Wadler, S., Otter, B. A. (1994) Potentiation of the antitumor activity of 5-fluorouracil in colon carcinoma cells by the combination of interferon and deoxyribonucleosides results from complementary effects on thymidine phosphorylase. *Cancer Res*. **54**: 1472–1478

Shimabukuro, T., Matsuyama, H., Baba, Y., Jojima, K., Suyama, K. I., Aoki, A., Suga, A., Yamamoto, N., Naito, K. (2005) Expression of thymidine phosphorylase in human superficial bladder cancer. *Int. J. Urol*. **12**: 29–34

Takao, S., Takebayashi, Y., Che, X. M., Shinchi, H., Natsugoe, S., Miyadera, K., Yamada, Y., Akiyama, S., Aikou, T. (1998) Expression of thymidine phosphorylase is associated with a poor prognosis in patients with ductal adenocarcinoma of the pancreas. *Clin. Cancer Res*. **4**: 1619–1624

Takebayashi, Y., Akiyama, S., Akiba, S., Yamada, K., Miyadera, K., Sumizawa, T., Yamada, Y., Murata, F., Aikou, T. (1996) Clinicopathologic and prognostic significance of an angiogenic factor, thymidine phosphorylase, in human colorectal carcinoma. *J. Natl Cancer Inst*. **88**: 1110–1117

Toi, M., Rahman, M. A., Bando, H., Chow, L. W. C. (2005) Thymidine phosphorylase (platelet-derived endothelial-cell growth factor) in cancer biology and treatment. *Lancet Oncol*. **6**: 158–166

Yano, S., Kazuno, H., Suzuki, N., Emura, T., Wierzba, K., Yamashita, J., Tada, Y., Yamada, Y., Fukushima, M., Asao, T. (2004a) Synthesis and evaluation of 6-methylene-bridged uracil derivatives. Part 1: discovery of novel orally active inhibitors of human thymidine phosphorylase. *Bioorg. Med. Chem*. **12**: 3431–3441

Yano, S., Kazuno, H., Sato, T., Suzuki, N., Emura, T., Wierzba, K., Yamashita, J., Tada, Y., Yamada, Y., Fukushima, M., Asao, T. (2004b) Synthesis and evaluation of 6-methylene-bridged uracil derivatives. Part 2: Optimization of inhibitors of human thymidine phosphorylase and their selectivity with uridine phosphorylase. *Bioorg. Med. Chem*. **12**: 3443–3450